POAC'23
Glasgow, United Kingdom

Proceedings of the 27th International Conference on
Port and Ocean Engineering under Arctic Conditions
12-16 June 2023, Glasgow, United Kingdom

Glacier Reconstruction on Anatolian Mountains Inferred from Ice flow Modelling

Adem Candaş[1,2], Mehmet Akif Sarıkaya[3], Ömer Lütfi Şen[3]
[1] Faculty of Mechanical Engineering, Istanbul Technical University, Istanbul, Türkiye
[2] PeriDynamics Research Centre, Department of Naval Architecture, Ocean and Marine Engineering, University of Strathclyde, Glasgow, UK
[3] Eurasia Institute of Earth Sciences, Istanbul Technical University, Istanbul, Türkiye

ABSTRACT

Climate change plays a fundamental role in the life cycle of glaciers. They melt under the current climatic crisis and contribute to the sea level rise. In order to know their current and past behaviours, they should be monitored or modelled under certain conditions. Reconstructions of past glaciers provide valuable information on future climate forecasts. Recent years have witnessed a growing academic interest in investigations of past glaciers and related climate data in Türkiye. Dating studies using cosmogenic isotopes is a key component of understanding the timing of paleoglaciers, especially for the Last Glacial Period (from 130k years earlier to 11k BP). Evidence from a number of dating studies has been established that these past glaciers in Anatolia have retreated from their maximum extents at 21ka to their minimal present conditions. The maximum glacier extent may have occurred much earlier in some regions in Türkiye, such as the Eastern Black Sea Mountains. The aim of this study is to develop a better understanding of the behaviour of glaciers in the Eastern Black Sea Mountains using physical based glacier modelling. We used the Parallel Ice Sheet Model (PISM) for paleoglacier reconstructions. The model's primary inputs are paleo- temperature and precipitation conditions. To do this, the current climatic conditions were used as a base pattern and modified to calculate the paleo- ice mass balance. The maximum extent of the modelling glaciers is compared with the proxies from previous studies conducted in the field. Here, we present the preliminary results of the effect of the paleoclimatic conditions on modelled glaciers, and how they behaved for 130ka under changing climatic conditions.

KEY WORDS : Paleoclimate, Glacier reconstruction,

INTRODUCTION

In recent years, there has been an increase in efforts to investigate the presence of glaciers in Türkiye. Cosmogenic isotope dating studies provide significant information about paleoglaciers, particularly during the Last Glacial Period (Last Glacial Stage: from 120 ka ago to 11.7 ka ago). These studies have revealed that the Anatolian paleoglaciers primarily attained their maximum size during the Last Glacial Maximum (LGM, ~ 21 ka ago) and subsequently retreated to their current positions. However, in some regions, the maximum glacial conditions occurred much earlier, as observed in the Eastern Black Sea Mountains (Reber et al., 2014). The reason why the glaciers reached such a large size is not fully understood, but it is possible that local climatic conditions differed from other regions in Anatolia. The study of glaciation makes a significant contribution to our understanding of not only the Late Ice Age climate but also the present climate and environmental changes.

Examining the vanishing glaciers of today and undertaking a quantitative analysis of their paleorecords is crucial for improved climate predictions in the future. In the IPCC's fifth assessment report (AR5), it was noted that the global surface temperature has risen by 0.89°C since 1880 (IPCC, 2013). Glacier mass loss amounted to 335 ± 38 gigatons per year between 2006-2015 (IPCC, 2019). Similarly, studies conducted by Sarikaya (2012) and Azzoni et al. (2019, 2020) indicate that the Ağrı Ice Cap, Türkiye's largest glacier, has decreased in size by one-third in last 30 years.

Determining the extent of glaciation in a region is crucial for understanding the scale and timing of past climate changes. Moreover, accurate dating of glacial deposits is essential for identifying the timing and rate of these changes. To this end, numerous dating studies have been conducted in the Eastern Black Sea Mountains. The first of these, as mentioned above, was the study conducted by Akçar et al. (2007) in Kavron Valley. Utilizing 22 samples, moraines deposited 27.3 ± 1.7 ka were identified using the ^{10}Be isotope. The authors concluded that the Last Glacial Maximum (LGM: 21 ka) glaciation ended 19.8 ± 1.4 ka, Late Glacial period moraines were dated to 17.0 ± 1.1 ka, and the Younger Dryas was dated to 12.8 ± 1.0 ka in the region. Similar results were obtained by the same authors in another nearby valley (Akçar et al., 2008). Following the dating studies conducted using 19 samples in Verçenik Valley, it was observed that LGM glaciers had begun to retreat 27.5 ± 1.8 ka and retreated entirely by 20.3 ± 1.4 ka. Additionally, Late Glacial period moraines were also identified in Verçenik Valley dating back to 17.2 ± 1.2 ka (Akçar et al., 2008). The study conducted by Reber et al. (2014) in Başyayla Valley indicated that glaciers in the Eastern Black Sea region developed much earlier than previously thought. The authors dated the region's glaciers to have reached their maximum size 57.0 ± 3.5 ka, indicating that local glacial maximum conditions occurred much earlier than global conditions. Based on the available information, the present study aims to reconstruct paleoglaciers by developing models that simulate the climatic conditions of the relevant period.

Here, we used Parallel Ice Sheet Model (PISM v.2.0.4) (https://www.pism.io) (Bueler and Brown, 2009; Winkelmann et al., 2011), an open-source numerical ice flow program, to reconstruct paleoglaciers in the study area. PISM was initially used to model large ice sheets (~10^6–10^7 km^2) on Greenland (Habermann et al., 2017; Nielsen et al., 2018), Antarctic (Feldmann and Levermann, 2015; Kingslake et al., 2018), and Cordilleran ice sheets (Seguinot et al., 2014, 2016). The paleoglacier size in the study area is relatively small (14,000 km^2) compared to continental scale ice sheets. There is a large volume of published studies focusing on high-resolution alpine glaciers (Golledge et al., 2012; Becker et al., 2016; Jouvet et al., 2017; Seguinot et al., 2018; Imhof et al., 2019; Schmidt et al., 2020; Bavec and Depolli, 2022; Martin

et al., 2022; Yan et al., 2023). Moreover, we adapted PISM to reconstruct paleoglaciers in two mountains in Turkey: Dedegöl Mountain (Candaş, 2017; Candaş et al., 2020) and Karanfil Mountain (Ciner et al., 2018, 2022; Sarıkaya et al., 2019; Köse et al., 2022) in the Taurus Range and Velebit Mountain (Žebre et al., 2021) in Croatia. The resolutions of these model domains are ~100 m and the model areas cover 225 km^2, 50 km^2, and 543 km^2 respectively.

This study aimed to understand the paleoclimatic conditions in the Eastern Black Sea of Turkey by reconstructing paleoglaciers in the past. Specifically, we compared the paleo-ice extents obtained from numerical ice models using PISM to moraine boundaries observed during field studies. These moraine boundaries represent the latest maximum distance reached by the glacier in the past. In other words, since that time, the climate has begun to warm up. By comparing the glacier boundaries with the model results, we can gain insights into the temperature and precipitation conditions for this point during the Last Glacial Maximum (21 ka ago).

METHODOLOGY

The study's methodology is provided, which commences with an introduction to the model domain, followed by an exposition of the climatic datasets and the application of climate forcings. Additionally, the mass budget of a glacier, specifically surface mass balance, and the laws governing ice rheology and basal sliding are presented.

Model Domain

The present study concerns a model domain spanning approximately 14,000 km^2 (153.8 × 91.3 km), positioned between 40.389 and 41.298°N and 40.213 and 41.747°E, comprising 185 × 110 horizontal cells each of roughly 30 arc-seconds (~1 km) resolution. The vertical spacing in ice is uneven, between 26.500 m < dz < 173.500 m, comprised of 51 levels. WorldClim v2.1 Digital Elevation Model topography data are used. The modern topography is not altered due to the limited volume of modern glaciers in the mountain. However, the authors acknowledge that the paleo- and present topography could potentially differ, as a result of glacial erosion, deposition and post- glacial karstification. Glacio-isostatic processes were ignored since the model domain is considerably smaller compared to large ice sheets. Geothermal heat flux influences the basal ice temperature of a glacier. It is estimated at the Earth's surface and is related to the temperatures of the Earth's crust and upper mantle. For the study area, the geothermal heat flux value ranges between 76.710 and 89.800 W m^{-2} and was derived from the global dataset provided by Shapiro and Ritzwoller (2004).

Climate Data Sets and Climate Forcing

The input data for calculating the glacier mass balance consists of two primary variables: monthly mean temperature and precipitation. Temperature data were obtained from the WorldClim v2.1 database (www.worldclim.org), which are an interpolation of average monthly observations from weather stations between 1970 and 2000 (Fick and Hijmans, 2017). The spatial resolution of the WorldClim data is approximately 30 arc-seconds (~1 km). There exist various sources for precipitation data that were developed through different methods, each with varying resolutions and time coverage. To identify the most suitable data source for a specific region, comparisons must be made among these sources. Table 1 provides a list of climate sets utilized for the local or global scale, which includes precipitation datasets with different temporal intervals and resolutions.

Table 1. Precipitation data sources properties.

Data Name	Short Name	Horizontal Resolution (º) / Study Area (km)	Temporal Coverage / Study Area	Reference
ECMWF Reanalysis 5th Generation for Lands	ERA5-Land	0.1 x 0.1 / 9 x 9 km	From Jan.1950 /1970 - 2000	Hersbach et al. (2020)
ECMWF Reanalysis 5th Generation for Lands - bioclimatic indicators	ERA5-Bio12	0.008 x 0.008 / 0.8 x 0.8 km	From Jan.1979 /1979 - 2008	Wouter (2021)
Cimatologies at High Resolution for the Earth's Land Surface Areas	Chelsa	0.008 x 0.008 / 0.8 x 0.8 km	1979 - 2016 /1981 -2010	Karger et al. (2021)
The Precipitation Estimation from Remotely Sensed Information using Artificial Neural Networks - Dynamic Infrared Rain Rate near real-time	Persiann-PDIR	0.04 x 0.04 / 4 x 4 km	From Mar.2000 / 2000-2021	Nguyen et al. (2019)
Integrated Multi-satellitE Retrievals for GPM v.06	IMERG	0.1 x 0.1 / 9 x 9 km	From Jun. 2000 / 2000-2021	Huffman et al. (2020)
WorldClim v2.1	WorldClim	0.008 x 0.008 / 0.8 x 0.8 km	1970 - 2000 / 1970 - 2000	Fick and Hijmans (2017)
Asian Precipitation - Highly-Resolved Observational Data Integration Towards Evaluation of Water Resources	Aphrodite	0.25 x 0.25 / 24 x 24 km	From 1951 / 1970-2020	Yatagai et al. (2009)
Parameter-elevation Relationships on Independent Slopes Model	PRISM	0.05 x 0.05 / 4.5 x 4.5 km	From 1900 / 1970 -2005	Çağlar (2023) (Unpub.)
Turkish State Meteorological Service	MGM omgi	0.006 x 0.006 / 0.5 x 0.5 km	From 1900 / 2010-2019	Mevbis (2022)

To simulate the climatic conditions during the Last Glacial Maximum (LGM), we introduced modifications to the present-day climate data. Specifically, we applied temperature and precipitation modifications to today's climate inputs. To build the colder LGM climate, the monthly temperatures were reduced by a temperature offset (ΔT: −9, −10, and −11°C). To represent the changes in precipitation, we used correction factors, known as precipitation multipliers ($\times P_{mult.}$: 0.75, 1, and 1.25), which ranged from 25% drier to 25% wetter than the present-day conditions. These modifications allowed us to recreate the climate conditions at the time of maximum glacial extent during the LGM.

$$T_{paleo}(x, y) = T_{present}(x, y) + \Delta T \quad (1)$$

$$P_{paleo}(x, y) = P_{present}(x, y) \times P_{mult.} \quad (2)$$

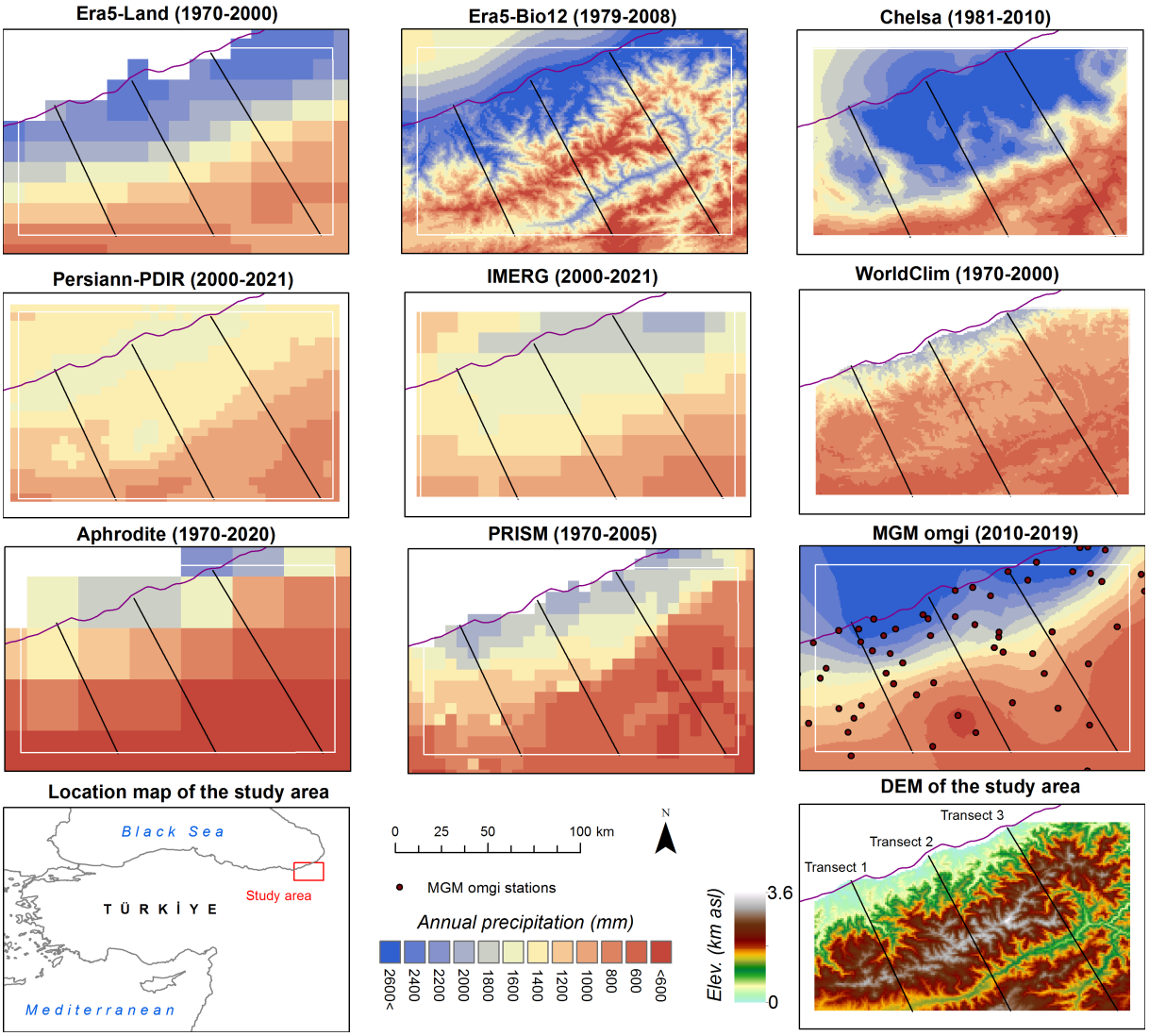

Figure 1. Annual precipitation comparison of climate data sets in the Eastern Black Sea Mountains

Surface Mass Balance

The surface mass balance, which refers to the difference between ice accumulation and ablation, plays a vital role in determining the yearly budget of a glacier at a given time and location (Becker et al., 2016). It is crucial to take into account the input-output relationship of snow, firn, and ice over a year for calculating the surface mass balance. Accumulation is defined as the addition of water-equivalent ice and/or snow to a glacier, and for this study, we assumed that accumulation occurred only through direct snowfall since other terms of accumulation are limited in the study area. Ablation, on the other hand, refers to the removal of snow and/or ice from a glacier.

To calculate the spatial distribution of paleo-surface mass balance, the model requires monthly mean temperature and precipitation values. We used prescribed temperature offsets and precipitation multipliers to modify the present-day climate values to reconstruct the climate conditions during the maximum glacial extent of the LGM. Ice accumulation was calculated based on the amount of precipitation that falls within the study area. If precipitation occurs at

air temperatures below 0°C, all precipitation was considered snowfall and was converted to water-equivalent ice to contribute to glacier mass balance. The contribution of snow accumulation linearly decreases from 0 to 2°C and does not contribute above 2°C (Becker et al., 2016). The melt-water refreeze factor (*rf*) was chosen as zero, meaning there is no ice contribution from refreezing melt.

To calculate glacier ablation, we employed the positive degree day (PDD) model as proposed by Braithwaite (1995). This widely used method is based on the yearly sum of PDD at the surface, which empirically provides the melting amount of a glacier (Wake and Marshall, 2015). The PDD model assumes that there is a correlation between the sum of temperatures above the melting point of snow and/or ice and the amount of observed melt at the same location over a certain period. We chose PDD factors of 3.2967 and 8.79121 mm day^{-1} °C^{-1} for snow (*ddfs*) and ice (*ddfi*), respectively (Braithwaite, 1995; Zweck and Huybrechts, 2005). As we did not have exact PDD values for our study area, we calculated the expected positive degree days (EPPD) using the equation provided by Zweck and Huybrechts (2005).

$$\mathrm{EPDD} = \sigma \int_1^{12} 30.4 \left[0.3989 \exp\left(-1.58 \left| \frac{T_i}{\sigma} \right|^{1.1372} \right) + \max\left(0, \frac{T_i}{\sigma}\right) \right] dt, \quad (3)$$

where T_i is the monthly air temperature near a surface and σ is the standard deviation of monthly temperature considering the daily cycle. It is imported from WorldClim v2.1 BIO4 dataset for the study area. We have previously demonstrated that the EPDD-PDD difference calculated using data from nearby stations was up to 2.1% (Candaş et al., 2020).

Ice rheology and Basal Sliding

In this study, the PISM model is utilized to employ a hybrid stress approximation founded on both the shallow-ice (SIA) (Hutter, 1983) and shallow-shelf approximation (SSA) (Morland, 1987; Winkelmann et al., 2011). SIA is typically implemented in continental scale ice sheet simulations, where the primary effect dictating ice flow is the internal shear stress of the ice. SIA is a suitable model for simulating ice sheets as it is particularly well-suited for areas with shallow bed surfaces and relatively small thickness to length ratios. On the other hand, the hybrid stress approximation, SIA + SSA, has proven to be effective in simulating the New Zealand Southern Alps (Golledge et al., 2012), the European Alps (Becker et al., 2016; Jouvet et al., 2017), Anatolian Mountains (Candaş et al., 2020; Köse et al., 2022), and Velebit Mountain in Croatia (Žebre et al., 2021) allowing for sliding to be incorporated into internal ice flow in mountainous areas (Bueler and Brown, 2009). The relationship between stress and deformation of the glacier is defined by the Glen-Paterson-Budd-Lliboutry-Duval flow law (Lliboutry and Duval, 1985), which is an enthalpy-based default in PISM (Aschwanden et al., 2012). The strain rate is:

$$\dot{\epsilon}_{ij} = \mathrm{E} \cdot A(T, \omega) \tau_e^{n-1} \boldsymbol{\tau}_{ij}, \quad (4)$$

where E is the enhancement factor, $A(T, \omega)$ is ice softness, which is a function of liquid water fraction ω and temperature T, n is the Glen's flow law exponent, τ_e is the effective stress,

and $\boldsymbol{\tau}_{ij}$ is the deviatoric stress tensor (Albrecht et al., 2020). Table 2 presents a summary of the ice flow parameters and the corresponding climatic forcings.

Table 2. Physical constants and parameters used in the glacier modelling

Parameter	Name	Value	Unit	Reference
Ice and Earth dynamics				
g	Gravitational acceleration	9.81	m s^{-2}	-
ρ_b	Bedrock density	3300	kg m^{-3}	-
q_G	Geothermal heat flux	70.42	W m^{-2}	Shapiro and Ritzwoller (2004)
ρ	Ice Density	910	kg m^{-3}	Aschwanden et al. (2012)
n	Exponent in Glen's flow law	3		Cuffey and Paterson (2010)
E_{SIA}	SIA enhancement factor	1		-
E_{SSA}	SSA enhancement factor	1		-
Basal sliding and subglacial hydrology				
q (PPQ)	Pseudo-plastic sliding exponent	0.25	-	Aschwanden et al. (2013)
$u_{threshold}$	Pseudo-plastic threshold velocity	100	m a^{-1}	Aschwanden et al. (2013)
c_0	Till cohesion	0	Pa	Tulaczyk et al. (2000)
ϕ	Till friction angle	30	°	Cuffey and Paterson (2010)
W_{max}	Maximum till water thickness	2	m	Bueler and van Pelt (2015)
e_0	Till reference void ratio	1	-	Tulaczyk et al. (2000)
C_c	Till compressibility coefficient	0.12	-	Tulaczyk et al. (2000)
δ	Till effective fraction overburden	0.02	-	Bueler and van Pelt (2015)
N_0	Till reference effective pressure	1000	Pa	Tulaczyk et al. (2000)
Climate forcings				
T_s	Temperature of snow precipitation	0	°C	Seguinot et al. (2018)
T_r	Temperature of rain precipitation	2	°C	Seguinot et al. (2018)
ddfi	Degree-day factor for ice	8.79121	mm day^{-1} $°C^{-1}$	
ddfs	Degree-day factor for snow	3.2967	mm day^{-1} $°C^{-1}$	
rf	Refreezing factor	0	-	

PISM incorporates a basal sliding law with a power q value as follows (Bueler and Brown, 2009; Greve and Blatter, 2009; Cuffey and Paterson, 2010)

$$\tau_b = -\tau_C \frac{\mathbf{u}}{u_{threshold}^q |\mathbf{u}|^{1-q}}, \quad (5)$$

where τ_b is the basal shear stress, τ_c yield stress. $u_{threshold}$ is a parameter that defines the limit velocity. When the parameter q is equal to zero, the power law is considered as purely-plastic (Coulomb), in the presence of a non-zero value for the power depending of which date

set, both the threshold velocity and power q govern the plasticity of ice. It is important to note that sliding can only occur once the basal stress surpasses the yield stress, which is determined using the Mohr-Coulomb criterion:

$$\tau_c = c_o + (\tan \phi) N_{till}, \tag{6}$$

where c_0 is the till cohesion and ϕ is the till friction angle. N_{till} is the effective pressure on the saturated till and the following expression is used to represent it:

$$N_{till} = min\left\{P_o, N_0 \left(\frac{\delta P_o}{N_0}\right)^s 10^{(e_0/C_c)(1-s)}\right\}, \tag{7}$$

where $P_o = \rho g H$ is the overburden pressure governing by ice thickness and ice density. The power s is the proportion of the effective thickness of water in the till W_{till} and the maximum amount of water in the till W_{max}. The variable δ represents the effective fraction of the till's overburden. In PISM's subglacial hydrology model, which follows the "undrained plastic bed" approach (Tulaczyk et al., 2000), the amount of water present in the till is directly linked to the basal melt rate calculated in PISM's energy conservation model.

RESULTS

We compare the model output of eight climate input data sets. To enable a fair comparison of precipitation data sets, the same temperature offset of ΔT: −10 °C is applied, while keeping the precipitation constant at present-day values ($\times P_{mult.}$: 1). The simulations were run until steady-state conditions in terms of volume were achieved, which took about 1500 years for all models to pass through the transient zone (Fig 2).

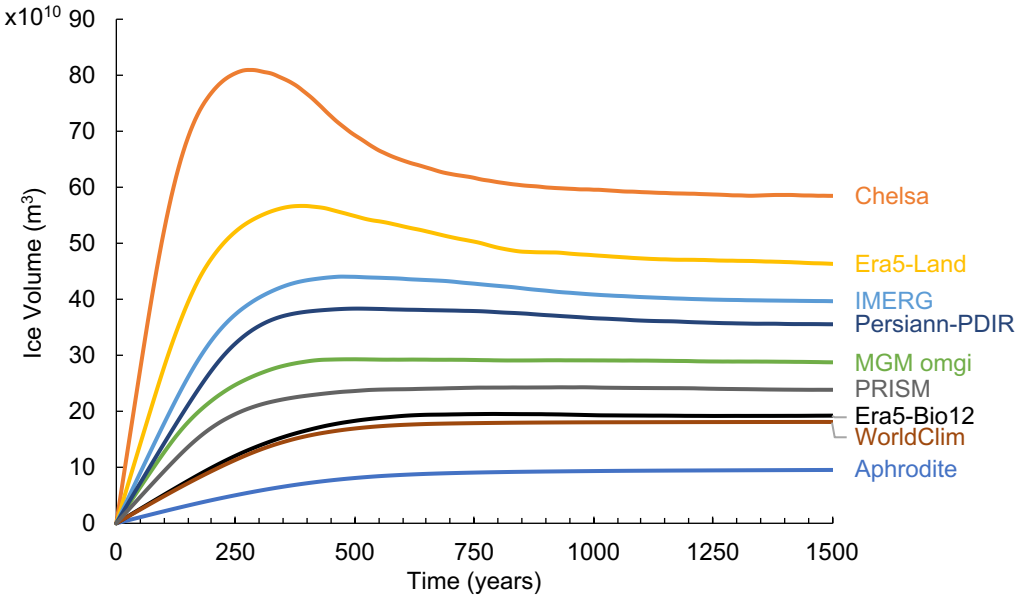

Figure 2. (a) Glacier volume over 1500 years

The land glacier volume and area are presented in Figure 2 and Figure 3, respectively, which show that glacier area exhibits a more rapid response to changes in climate compared to volume. These results are in agreement with Golledge et al.'s, (2012) findings which showed the response of glacier area and volume to climate perturbations. This phenomenon can be attributed to the immediate reduction of equilibrium line altitude (ELA) in response to cooling, whereas an increase in volume relies on precipitation and net accumulation rates. All of the simulations were subjected to the same temperature offset of ΔT, resulting in the same equilibrium line altitude (ELA). However, there were variations in the precipitation inputs among the different models depending on date set used.

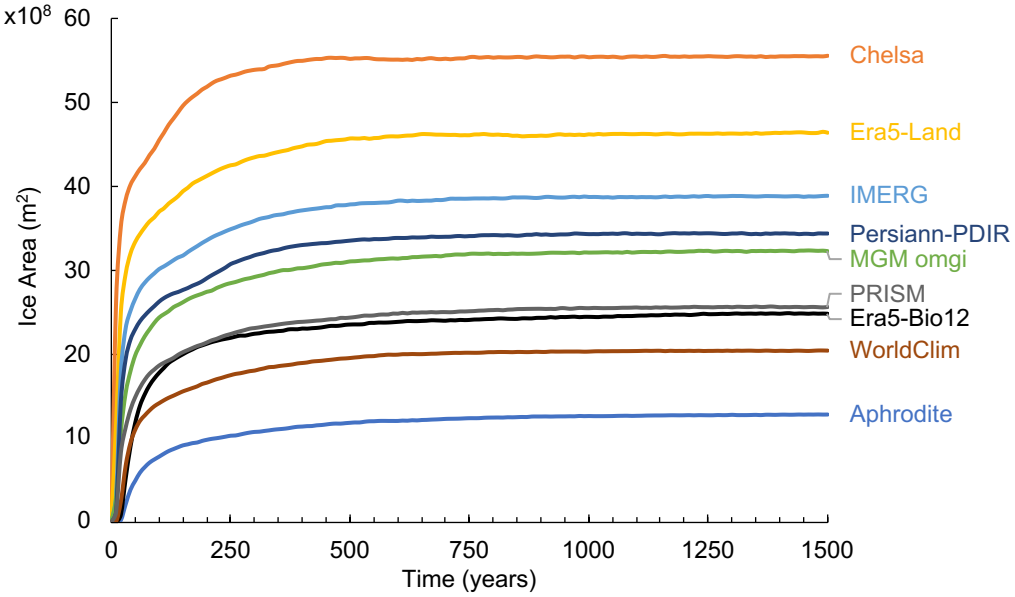

Figure 3. Ice area change starting from ice free conditions

Figure 4 depicts the PISM modelled ice thickness and coverage in the study area, in response to paleoclimate forcing. The climatic modifiers are temperature offset, ΔT: -10°C and precipitation changes, $\times P_{mult.}$: 1. The study covers a total area of 140 $\times 10^8$ m^2 with a horizontal resolution of approximately 1 km. The results show that the Chelsa dataset has the maximum glacier area and volume, while the Aphrodite dataset results in the smallest ice coverage. The MGM omgi dataset is obtained from the Turkish State Meteorological Service's Automatic Weather Observing Stations (AWOS) and may be considered to be the best precipitation data available. However, it has some limitations. Since these stations were mostly established right before 2010 in the region, the time range only covers the period from 2010 to 2019, which is a relatively short period for climate data. Additionally, the dataset is based on point data collected from stations with elevations ranging from sea level to 2666 m, and these data are then interpolated to match the topography and temperature data using Kriging method embedded in the ArcGIS program. While Kriging is useful for predicting values at unmeasured locations, as shown in Figure 1, the interpolated MGM data is not still very compatible with the topography and therefore not suitable for direct use in simulations. Among the other precipitation input sets listed in Table 1, datasets with high spatial resolution and compatibility with the topography should be evaluated. These reanalysed datasets can be compared with station data. The MGM dataset provides data from 112 stations. Nine stations located above an altitude of 1000 m were compared with other datasets. The WorlClim and Persiann-PDIR datasets stand out as being most compatible with the station data for the study area.

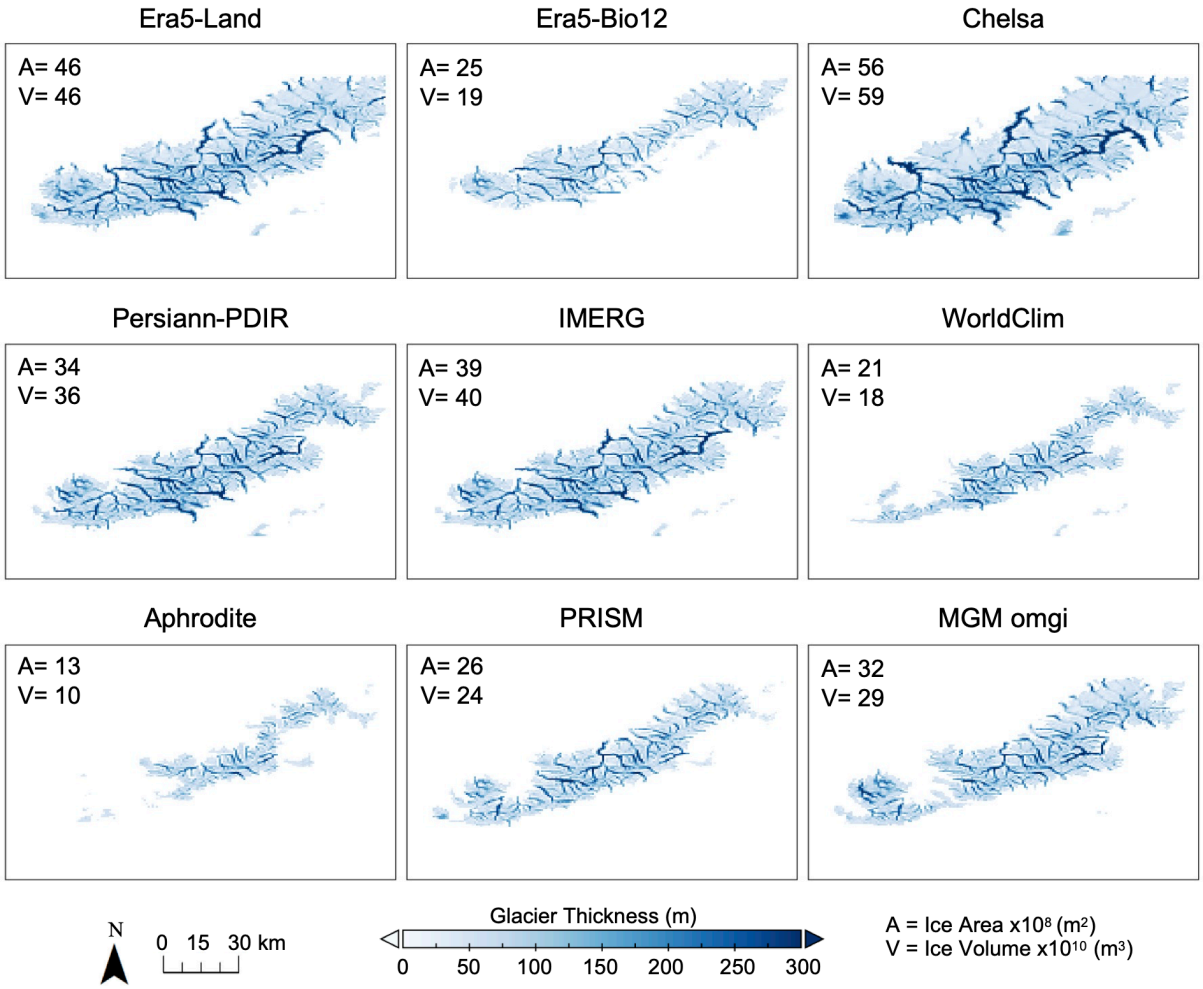

Figure 4. PISM modelled ice thickness (ΔT: −10 °C, $\times P_{mult.}$: 1)

CONCLUSIONS

Several mountains in Anatolia were glaciated during the Late Quaternary. In this study, we used the PISM to simulate paleo-glaciers in East Black Sea Mountains using various precipitation data sources. The numerical ice-flow model was forced by temperature offset of ΔT: −10 °C. The findings of this study serve as an input for comparison with the moraine boundaries determined in field studies. By comparing the maximum glacial extents obtained from the simulations with the observed moraine boundaries, we can determine which climate data set is best suited for this study area.

ACKNOWLEDGEMENTS

Adem Candaş is supported by the Scientific and Technological Research Council of Turkey (TÜBİTAK) 2219 International Postdoctoral Research Fellowship Program, Project No: 1059B192100891. This work is supported by TÜBİTAK Project No: 121Y507. Development of PISM is supported by NSF grants PLR-1644277 and PLR-1914668 and NASA grants NNX17AG65G and 20-CRYO2020-0052.

REFERENCES

Akçar, N., Yavuz, V., Ivy-Ochs, S., Kubik, P.W., Vardar, M. & Schlüchter, C., 2007. Paleoglacial records from Kavron Valley, NE Turkey: Field and cosmogenic exposure dating evidence. *Quaternary International*, 164–165, pp. 170–183. https://doi.org/10.1016/j.quaint.2006.12.020.

Akçar, N., Yavuz, V., Ivy-Ochs, S., Kubik, P.W., Vardar, M. & Schlüchter, C., 2008. A case for a downwasting mountain glacier during Termination I, Verçenik valley, northeastern Turkey. *Journal of Quaternary Science*, 23(3), pp. 273–285. https://doi.org/10.1002/jqs.1144.

Albrecht, T., Winkelmann, R. & Levermann, A., 2020. Glacial-cycle simulations of the Antarctic Ice Sheet with the Parallel Ice Sheet Model (PISM)-Part 1: Boundary conditions and climatic forcing. *Cryosphere*, 14(2), pp. 599–632. https://doi.org/10.5194/tc-14-599-2020.

Aschwanden, A., Aøalgeirsdóttir, G. & Khroulev, C., 2013. Hindcasting to measure ice sheet model sensitivity to initial states. *Cryosphere*, 7(4), pp. 1083–1093. https://doi.org/10.5194/tc-7-1083-2013.

Aschwanden, A., Bueler, E., Khroulev, C. & Blatter, H., 2012. An enthalpy formulation for glaciers and ice sheets. *Journal of Glaciology*, 58(209), pp. 441–457. https://doi.org/10.3189/2012JoG11J088.

Azzoni, R.S., Sarıkaya, M.A. & Fugazza, D., 2020. Turkish glacier inventory and classification from high-resolution satellite data. *Mediterranean Geoscience Reviews*, 2(1), pp. 153–162. https://doi.org/10.1007/s42990-020-00029-2.

Azzoni, R.S. … Zerboni, A., 2019. Geomorphological effects of the 1840 Ahora Gorge catastrophe on Mount Ararat (Eastern Turkey). *Geomorphology*, 332, pp. 10–21. https://doi.org/10.1016/j.geomorph.2019.02.001.

Bavec, A. & Depolli, M., 2022. Alpine glacier simulation with linear climate models. in *2022 45th Jubilee International Convention on Information, Communication and Electronic Technology, MIPRO 2022 - Proceedings*, pp. 245–250. https://doi.org/10.23919/MIPRO55190.2022.9803326.

Becker, P., Seguinot, J., Jouvet, G. & Funk, M., 2016. Last Glacial Maximum precipitation pattern in the Alps inferred from glacier modelling. *Geogr. Helv.*, 71(3), pp. 173–187. https://doi.org/10.5194/gh-71-173-2016.

Braithwaite, R.J., 1995. Positive Degree-Day Factors for Ablation on the Greenland Ice-Sheet Studied by Energy-Balance Modeling. *Journal of Glaciology*, 41(137), pp. 153–160. internal-pdf://77.147.216.47/Braithwaite-1995-Positive Degree-Day Factors f.pdf.

Bueler, E. & Brown, J., 2009. Shallow shelf approximation as a 'sliding law'" in a thermomechanically coupled ice sheet model'. *Journal of Geophysical Research-Earth Surface*, 114. https://doi.org/Artn F03008 10.1029/2008jf001179.

Bueler, E. & Van Pelt, W., 2015. Mass-conserving subglacial hydrology in the Parallel Ice Sheet Model version 0.6. *Geoscientific Model Development*, 8(6), pp. 1613–1635. https://doi.org/10.5194/gmd-8-1613-2015.

Candaş, A., 2017. *Reconstruction of the Paleoclimate on Dedegöl Mountain With Paleoglacial Records and Numerical Ice Flow Models*. Master Thesis, Eurasia Institute of Earth Sciences, Istanbul Technical University.

Candaş, A., Sarıkaya, M.A., Köse, O., Şen, Ö.L. & Çiner, A., 2020. Modelling Last Glacial

Maximum ice cap with the Parallel Ice Sheet Model to infer palaeoclimate in south-west Turkey. *Journal of Quaternary Science*, 35(7), pp. 935–950. https://doi.org/10.1002/jqs.3239.

Ciner, A., Sarıkaya, M.A., Köse, O., Candaş, A., Yıldırım, C. & Wilcken, K., 2022. Cosmogenic 36Cl glacial chronology and ice-flow modelling (PISM) of Aladağ and Karanfil Mountains, Central Taurus Range, Turkey. in *10th International Conference on Geomorphology, ICG2022-39*. 12–16 Sep 2022, Coimbra, Portugal. https://doi.org/doi.org/10.5194/icg2022-39, 2022.

Ciner, A., Köse, O., Sarıkaya, M.A., Yıldırım, C., Candaş, A. & Wilcken, K.M., 2018. Late Pleistocene Cosmogenic 36Cl Glacial Chronology of the Mount Karanfil, Central Taurus Range, Turkey. in *AGU Fall Meeting Abstracts*, pp. EP53F-1958. https://ui.adsabs.harvard.edu/abs/2018AGUFMEP53F1958C.

Cuffey, K.M. & Paterson, W.S.B., 2010. *The physics of glaciers, 4th Edition*. *Elsevier*. https://doi.org/10.1016/0016-7185(71)90086-8.

Feldmann, J. & Levermann, A., 2015. Collapse of the West Antarctic Ice Sheet after local destabilization of the Amundsen Basin. *Proceedings of the National Academy of Sciences*, 112(46), pp. 14191–14196. https://doi.org/10.1073/pnas.1512482112.

Fick, S.E. & Hijmans, R.J., 2017. WorldClim 2: new 1-km spatial resolution climate surfaces for global land areas. *International Journal of Climatology*, 37(12), pp. 4302–4315. https://doi.org/10.1002/joc.5086.

Golledge, N.R. … Schaefer, J.M., 2012. Last Glacial Maximum climate in New Zealand inferred from a modelled Southern Alps icefield. *Quaternary Science Reviews*, 46, pp. 30–45. https://doi.org/10.1016/j.quascirev.2012.05.004.

Greve, R. & Blatter, H., 2009. *Dynamics of Ice Sheets and Glaciers*. *Dynamics of Ice Sheets and Glaciers*. https://doi.org/10.1007/978-3-642-03415-2.

Habermann, M., Truffer, M. & Maxwell, D., 2017. Error sources in basal yield stress inversions for Jakobshavn Isbræ, Greenland, derived from residual patterns of misfit to observations. *Journal of Glaciology*, 63(242), pp. 999–1011. https://doi.org/10.1017/jog.2017.61.

Hersbach, H. … Thépaut, J.N., 2020. The ERA5 global reanalysis. *Quarterly Journal of the Royal Meteorological Society*, 146(730), pp. 1999–2049. https://doi.org/10.1002/qj.3803.

Huffman, G.J. … Xie, P., 2020. Integrated Multi-satellite Retrievals for the Global Precipitation Measurement (GPM) Mission (IMERG). in *Advances in Global Change Research*. Springer, pp. 343–353. https://doi.org/10.1007/978-3-030-24568-9_19.

Hutter, K., 1983. *Theoretical glaciology: material science of ice and the mechanics of glaciers and ice sheets*. *Journal of Glaciology*.

Imhof, M.A., Cohen, D., Seguinot, J., Aschwanden, A., Funk, M. & Jouvet, G., 2019. Modelling a paleo valley glacier network using a hybrid model: An assessment with a Stokes ice flow model. *Journal of Glaciology*, 65(254), pp. 1000–1010. https://doi.org/10.1017/jog.2019.77.

IPCC, 2013. *Climate Change 2013: Synthesis Report. (Contribution of working groups I, II and III to the fourth assessment report of the Intergovernmental Panel on Climate Change)*. Geneva, Switzerland.

IPCC, 2019. *IPCC Special Report on the Ocean and Cryosphere in a Changing Climate". Technical Summary*. Geneva, Switzerland.

Jouvet, G., Seguinot, J., Ivy-Ochs, S. & Funk, M., 2017. Modelling the diversion of erratic boulders by the Valais Glacier during the last glacial maximum. *Journal of Glaciology*, 63(239), pp. 487–498. https://doi.org/10.1017/jog.2017.7.

Karger, D.N., Wilson, A.M., Mahony, C., Zimmermann, N.E. & Jetz, W., 2021. Global daily 1 km land surface precipitation based on cloud cover-informed downscaling. *Scientific Data*, 8(1), pp. 1–18. https://doi.org/10.1038/s41597-021-01084-6.

Kingslake, J. … Whitehouse, P.L., 2018. Extensive retreat and re-advance of the West Antarctic Ice Sheet during the Holocene. *Nature*, 558(7710), pp. 430–434. https://doi.org/10.1038/s41586-018-0208-x.

Köse, O., Sarıkaya, M.A., Çiner, A., Candaş, A., Yıldırım, C. & Wilcken, K.M., 2022. Reconstruction of Last Glacial Maximum glaciers and palaeoclimate in the central Taurus Range, Mt. Karanfil, of the Eastern Mediterranean. *Quaternary Science Reviews*, 291, p. 107656. https://doi.org/10.1016/j.quascirev.2022.107656.

Lliboutry, L. & Duval, P., 1985. Various isotropic and anisotropic ices found in glaciers and polar ice caps and their corresponding rheologies. in *International Journal of Rock Mechanics and Mining Sciences & Geomechanics Abstracts*, p. 198. https://doi.org/10.1016/0148-9062(85)90267-0.

Martin, J., Davies, B.J., Jones, R. & Thorndycraft, V., 2022. Modelled sensitivity of Monte San Lorenzo ice cap, Patagonian Andes, to past and present climate. *Frontiers in Earth Science*, 10. https://doi.org/10.3389/feart.2022.831631.

Mevbis, 2022. *Meteorolojik Bilgi Satış ve Sunum Sistemi (MEVBİS)*.

Morland, L.W., 1987. Unconfined ice-shelf flow. in *Dynamics of the West Antarctic Ice Sheet: Proceedings of a Workshop held in Utrecht, May 6–8, 1985*. Springer, pp. 99–116.

Nguyen, P. … Sorooshian, S., 2019. The CHRS data portal, an easily accessible public repository for PERSIANN global satellite precipitation data. *Scientific Data*, 6(1), pp. 1–10. https://doi.org/10.1038/sdata.2018.296.

Nielsen, L.T., Adalgeirsdóttir, G., Gkinis, V., Nuterman, R. & Hvidberg, C.S., 2018. The effect of a Holocene climatic optimum on the evolution of the Greenland ice sheet during the last 10 kyr. *Journal of Glaciology*, 64(245), pp. 477–488. https://doi.org/10.1017/jog.2018.40.

Reber, R. … Schlüchter, C., 2014. Glacier advances in northeastern turkey before and during the global last glacial maximum. *Quaternary Science Reviews*, 101, pp. 177–192. https://doi.org/10.1016/j.quascirev.2014.07.014.

Sarıkaya, M.A., 2012. Recession of the ice cap on Mount Aĝri (Ararat), Turkey, from 1976 to 2011 and its climatic significance. *Journal of Asian Earth Sciences*, 46, pp. 190–194. https://doi.org/10.1016/j.jseaes.2011.12.009.

Sarıkaya, M.A., Candaş, A., Köse, O., Şen, Ö.L., Çiner, A. & Wilcken, K.M., 2019. Late Pleistocene Cosmogenic 36Cl Glacial Geochronology and PISM Ice Flow Model of the Central Taurus. in *International Symposium on Geomorphology 2019*. Ankara, Turkey.

Schmidt, L.S., Aoalgeirsdóttir, G., Pálsson, F., Langen, P.L., Guomundsson, S. & Björnsson, H., 2020. Dynamic simulations of Vatnajökull ice cap from 1980 to 2300. *Journal of Glaciology*, 66(255), pp. 97–112. https://doi.org/10.1017/jog.2019.90.

Seguinot, J., Rogozhina, I., Stroeven, A.P., Margold, M. & Kleman, J., 2016. Numerical simulations of the Cordilleran ice sheet through the last glacial cycle. *Cryosphere*, 10(2), pp.

639–664. https://doi.org/10.5194/tc-10-639-2016.

Seguinot, J., Ivy-Ochs, S., Jouvet, G., Huss, M., Funk, M. & Preusser, F., 2018. Modelling last glacial cycle ice dynamics in the Alps. *Cryosphere*, 12(10), pp. 3265–3285. https://doi.org/10.5194/tc-12-3265-2018.

Seguinot, J., Khroulev, C., Rogozhina, I., Stroeven, A.P. & Zhang, Q., 2014. The effect of climate forcing on numerical simulations of the cordilleran ice sheet at the last glacial maximum. *Cryosphere*, 8(3), pp. 1087–1103. https://doi.org/10.5194/tc-8-1087-2014.

Shapiro, N.M. & Ritzwoller, M.H., 2004. Inferring surface heat flux distributions guided by a global seismic model: particular application to Antarctica. *Earth and Planetary Science Letters*, 223(1–2), pp. 213–224.

Tulaczyk, S., Kamb, W.B. & Engelhardt, H.F., 2000. Basal mechanics of Ice Stream B, west Antarctica: 2. Undrained plastic bed model. *Journal of Geophysical Research: Solid Earth*, 105(B1), pp. 483–494.

Wake, L.M. & Marshall, S.J., 2015. Assessment of current methods of positive degree-day calculation using in situ observations from glaciated regions. *Journal of Glaciology*, 61(226), pp. 329–344. https://doi.org/10.3189/2015JoG14J116.

Winkelmann, R. … Levermann, A., 2011. The Potsdam Parallel Ice Sheet Model (PISM-PIK) - Part 1: Model description. *Cryosphere*, 5(3), pp. 715–726. https://doi.org/10.5194/tc-5-715-2011.

Wouter, K., 2021. *Global bioclimatic indicators from 1979 to 2018 derived from reanalysis*. *Copernicus Climate Change Service (C3S) Climate Data Store (CDS)*. https://doi.org/10.24381/cds.bce175f0.

Yan, Q., Owen, L.A., Guo, C., Zhang, Z., Zhang, J. & Wang, H., 2023. Widespread glacier advances across the Tian Shan during Marine Isotope Stage 3 not supported by climate-glaciation simulations. *Fundamental Research*, 3(1), pp. 102–110. https://doi.org/10.1016/j.fmre.2022.01.033.

Yatagai, A., Arakawa, O., Kamiguchi, K., Kawamoto, H., Nodzu, M.I. & Hamada, A., 2009. A 44-year daily gridded precipitation dataset for Asia based on a dense network of rain gauges. *Scientific Online Letters on the Atmosphere*, 5(1), pp. 137–140. https://doi.org/10.2151/sola.2009-035.

Žebre, M. … Wilcken, K.M., 2021. An early glacial maximum during the last glacial cycle on the northern Velebit Mt. (Croatia). *Geomorphology*, 392, p. 107918. https://doi.org/10.1016/j.geomorph.2021.107918.

Zweck, C. & Huybrechts, P., 2005. Modeling of the northern hemisphere ice sheets during the last glacial cycle and glaciological sensitivity. *Journal of Geophysical Research Atmospheres*, 110(7), pp. 1–24. https://doi.org/10.1029/2004JD005489.